STATISTICAL IMAGE SHARPENING

Carlo Grillenzoni

Dipartimento di Pianicazione, Università IUAV di Venezia, Italy
Email: carlog@iuav.it (submitted Sept. 2006, accepted March 2007).

Summary

Several methods of image enhancement have been proposed in engineering literature. Their major problem is that they are designed by rules of thumb or subjective evaluation. This paper develops statistical techniques for the optimization of the image sharpening. The most relevant feature is the automatic tuning of the parameter which controls the gradient addition. The approach is based on statistical measures which establish a trade-o between smoothness and sharpness. More generally, unsharp masks can be replaced by spatial autoregressive (SAR) models, and their coefficients can be estimated with adaptive and nonparametric approaches. Numerical applications to real case studies show the validity of the methods.

Keywords: Edge Detection, Image Enhancement, Kernel Densities, Least Squares, Normality Test, Spatial Autoregressive Models.

1. INTRODUCTION

Image enhancement provides numerical techniques which aim to improve the quality of digital images as they are perceived by the human eye. Contrary to computer vision methods, which attempt to extract from an image groups of objects, image enhancement focuses on the details and the totality of the image itself. In thiseld one can identify three main groups of techniques: (i) contrast balancing, which aims to equalize the pixel luminance and grey levels; (ii) noise removing, which attempts to delete sparse disturbances and scratches; and (iii) image sharpening, which tends to increase the boundaries between separate objects in the scene.

Engineering of image processing has developed several methods for dealing with these topics. They are respectively: Histogram equalization and Retinex techniques, e.g. Starck *et al.* (2003) and Funt *et al.* (2004). Smoothing methods and their edge-preserving versions, see Campbell *et al.* (1990) and Chu *et al.* (1998). Unsharp masking and their adaptive and nonlinear extensions, e.g. Guillon *et al.* (1999), Polesel *et al.* (2000) and Russo (2005). In many of these cases, the implemented filters suffer by the problem that tuning coefficients are designed following rules of thumb and subjective evaluation.

In this paper we are particularly concerned with image sharpening. The problem is the opposite one of image smoothing, because it aims to increase the edges of the image. The method of unsharp masking performs the task by adding to the original image a *portion* of the image gradient (usually computed by a Laplacian filter). This approach involves three fundamental issues: (1) How to tune the gradient portion ? (2) How to design the weights of the gradient filter ? (3) How to adapt these weights to local conditions ? These questions have been partly or totally unanswered in engineering literature, and in this paper, we shall provide some statistical solutions. Generally speaking, our methods focus on the optimization of statistics which balance the trade-off between sharpness and smoothness, and models which capture the spatial dependence between pixels.

The plan of the work is as follows: Section 2 deals with the problem of tuning the gradient portion in unsharp masking by using second and higher order statistics (autocorrelation, skewness and kurtosis). Section 3 develops sharpening filters based on spatial autoregressive models and discusses algorithms of adaptive and robust estimation. Throughout, an extended numerical application on a well known testing image is carried out.

2. OPTIMAL SHARPENING

Sharpening techniques aim to increase contrast at the boundaries of the objects present in the image. This enhances the perceived edges and details, although it doesn't increase the actual information content. Broadly speaking, these techniques perform the opposite action of smoothing. Thus, if Z_{ij} is the luminance of the pixel located in position ij, where $0 \leq Z \leq 255$ are the grey levels and $1 \leq i, j \leq n$ is the image size, then the sharpened solution $\check{Z}_{ij}$ is typically given by

$$\begin{aligned} \check{Z}_{ij} &= Z_{ij} + \alpha\, \hat{E}_{ij} \\ \hat{E}_{ij} &= (Z_{ij} - \hat{Z}_{ij}) \end{aligned} \tag{1}$$

where $\hat{Z}_{ij}$ is the smoothed (or unsharped) image, computed on a neighborhood of ij, and $0 < \alpha < \infty$ is a tuning constant.

Typically, the smoothed image is computed as arithmetic mean of the pixels located on and around ij. Using a 3×3 window, the equation (1) becomes

$$\check{Z}_{ij} = (1 + \alpha)\, Z_{ij} - \frac{\alpha}{9} \sum_{h=-1}^{1} \sum_{k=-1}^{1} Z_{i-h,j-k} \tag{2}$$

If the arithmetic mean avoids the 4 corner terms $Z_{i\pm1,j\pm1}$, and only considers the 5 (more adjacent) pixels, then the *edge* image $\hat{E}_{ij}$ coincides with the Laplacian gradient; namely, in the continuous space $\hat{E}(x, y) = \partial^2 Z(x, y)/\partial x\, \partial y$.

Apart from the choice of the smoother $\hat{Z}_{ij}$, the quality of the sharpening process crucially depends on the coefficient α. If its value is too high, then "grain effect" is introduced overall in the image, even in smooth regions where the gradient is negligible. Until now, only rules of thumb, such as subjective evaluation of the grain, have been suggested for designing α. To introduce statistical criteria, we now consider numerical experiments on the testing image "Lena".

It is a GIF image of size n=512 and range 0-255. Figure 1(a-d) displays the components $(Z, \hat{Z}, \hat{E}, \check{Z})$ of the equation (1) obtained with α=2.5 and a 3×3 averaging window. Significant insights on the effects produced by α can be obtained from the probability density $f_Z(z)$ of the pixel luminance in sharpened images. The kernel estimator is

$$\check{f}_Z(z_k|\alpha) = \frac{1}{n^2\, \lambda} \sum_{i=1}^{n} \sum_{j=1}^{n} K\left[\frac{\check{Z}_{ij}(\alpha) - z_k}{\lambda}\right], \qquad z_k = 0, 1, 2 \ldots 255 \tag{3}$$

Fig. 1: Components of equation (1) obtained with α=2.5 and a 3×3 window. Images: (a) Original Z; (b) Smoothed $\hat{Z}$; (c) Edge $\hat{E}$; (d) Sharpened $\check{Z}$.

where $K(\cdot)$ is a probability density and $0 < \lambda < \infty$ is a smoothing parameter. This can be designed as a function of the standard deviation (σ) of the pixel luminance; namely $\check{\lambda} = \check{\sigma}_Z/n^{1/5}$ (e.g. Härdle, 1991). Figure 2(a-d) shows kernel densities corresponding to sharpened images having α=0, 2.5, 5, 7.5 respectively. One can note that densities exhibit multimodality and, as the coefficient α increases, the overall dispersion rises significantly.

The results in Figure 2 suggest some statistical criteria to design the filters (1)-(2):

Solution 1. First note that as α increases, symmetry and unimodality of the kernel density tend to improve, but its flatness and dispersion worsen. This means that the optimal value of α may be the one which keeps $f_Z(z)$ as close as possible to a Gaussian density. In this context, a skewness-kurtosis statistic for Normality test can be employed to select α. Bera and Jarque (1982), using the Pearson family as the parametric alternative, derived a useful Lagrange multiplier test for time series. Adapting it to spatial data, provides

$$S_1(\alpha) = \left[\frac{n^2}{6}\left(\frac{\check{\mu}_3}{\check{\sigma}^3}\right)^2 + \frac{n^2}{24}\left(\frac{\check{\mu}_4}{\check{\sigma}^4} - 3\right)^2 \right] \tag{4}$$

where $\mu_c = \mathrm{E}[Z - \mathrm{E}(Z)]^c$ are central moments of order $c > 0$. Under the null hypothesis of Gaussianity the statistic (4) asymptotically has a chi-square distribution with 2 degrees of freedom. Even though all of the densities in Figure 2 reject the null hypothesis, namely $S_1(\alpha) > \chi^2_{.01}(2)$, the statistic (4) tends to have a well definite minimum with respect to α. Figure 4(a) exhibits this feature.

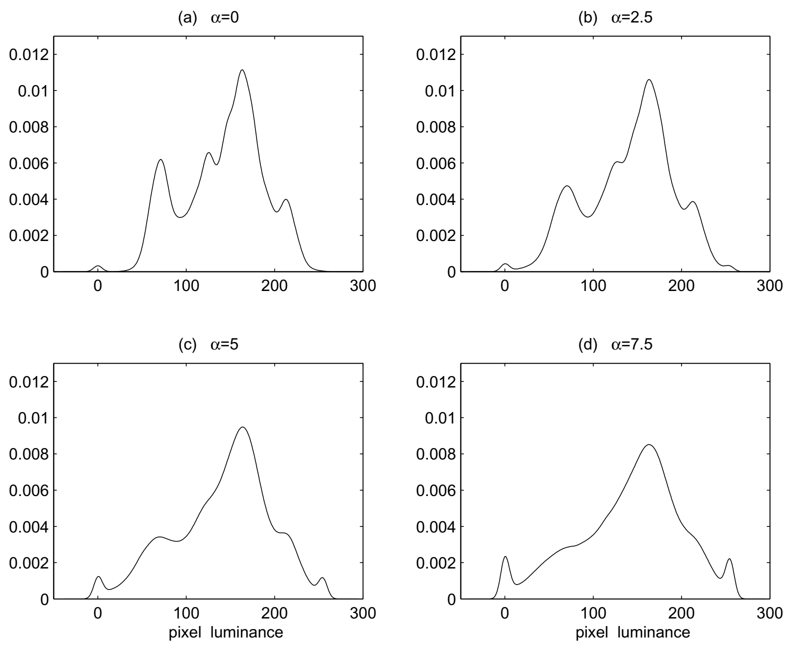

Fig. 2: Kernel density estimates of the pixel luminance of sharpened images with α=0, 2.5, 5, 7.5. They are obtained with formula (3) and $\lambda = \sigma_Z/n^{1/5}$.

Solution 2. The second approach only considers second order moments, such as variance and spatial autocovariances (ACV). For stationary processes the latter are defined as $\gamma_Z(h,k) = \mathrm{E}[\,Z_{ij}Z_{i-h,j-k}\,] - \mathrm{E}^2(Z_{ij})$, and measure the dependence between pixels which are separated by k-columns and h-rows. Because sharpening reduces smoothness, it also reduces spatial autocovariance and autocorrelation $\rho_Z = \gamma_Z/\sigma_Z^2$. This feature is shown in Figure 3, as concerned the one-sided functions $\check{\gamma}_Z(0,k), \check{\rho}_Z(0,k)$ computed on $\check{Z}_{ij}(\alpha)$. Indeed, as α increases, ρ_Z decreases for all $k > 0$.

On the other hand, the sharpening inflates the pixels' variance $\sigma^2 = \gamma(0,0)$; therefore, a statistic which sums Var and $\mathrm{ACV_s}$ should have a well definite maximum in α. Using unbiased sample autocovariances and a common lag $h = k$, one can define

$$\begin{aligned} S_2(\alpha|m) &= \sum_{k=(0,1)}^{m} \check{\gamma}_Z(k) \qquad (5) \\ \check{\gamma}_Z(k) &= (n-k)^{-2} \sum_{i=k+1}^{n} \sum_{j=k+1}^{n} (\check{Z}_{ij} - \bar{Z}_n)(\check{Z}_{i-k,j-k} - \bar{Z}_{n-k}) \end{aligned}$$

where $m \ll n$ is the maximum lag, and $\bar{Z}_{n-k}$ is the mean value computed on the sub-image with $i,j = (k+1)\ldots n$.

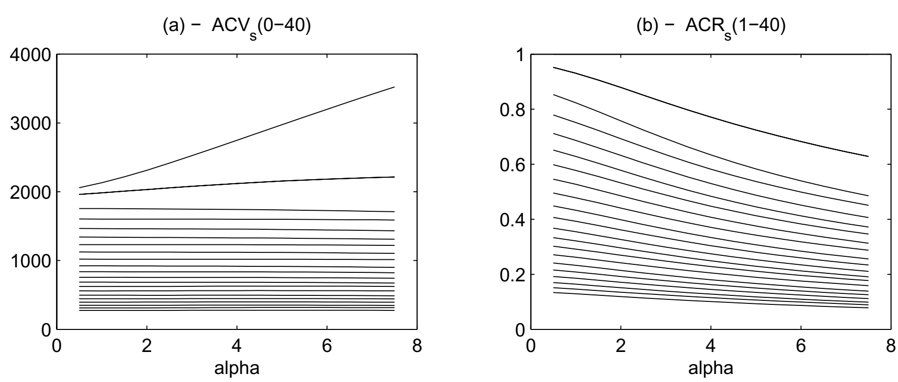

Fig. 3: Dependence between $\check{Z}_{ij}, \check{Z}_{i,j-k}$ in sharpened images with $0.5 \leq \alpha \leq 7.5$. (a) Autocovariances $\check{\gamma}_Z(0,k)$; (b) Autocorrelations $\check{\rho}_Z(0,k)$; with $k = 0,1,2,4\ldots40$.

In order to render strictly concave the statistic S_2, some specifications of (5) are required: i) First sum should start with $k = 1$ because the filter (2) includes the term $Z_{i-1,j-1}$. This renders the first autocovariance $\check{\gamma}_Z(1)$ increasing in α, that is a substitute for the variance $\check{\gamma}_Z(0)$, see Figure 3(a) below. ii) Because the autocovariance values depend on the texture of the image, the lag k could be defined only by row (with $\check{Z}_{i-k,j}$) or by column (with $\check{Z}_{i,j-k}$). Figures 4(c,d) show the behavior of the statistic (5) with these specifications.

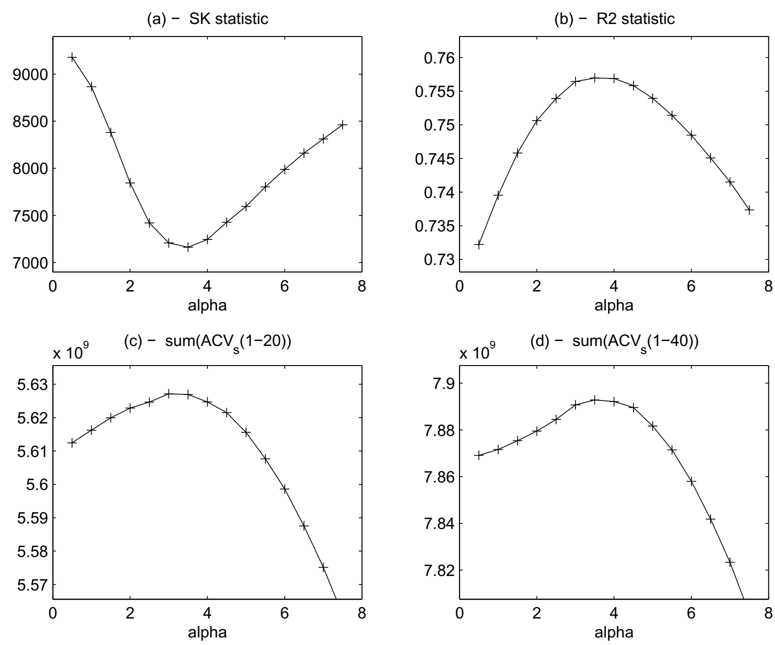

Fig. 4: Behavior of $S_{1,2,3}(\alpha)$, $0.5 \leq \alpha \leq 7.5$, in sharpened versions of Lena image: (a) Statistic (4); (b) Statistic (6); (c,d) Statistic (5) with $\check{\gamma}(0, k)$ and $m = 20, 40$.

Solution 3. The third statistic deals with the analysis of variance. Notice that sharpening transformation tends to increase the separation of the objects within the image, and therefore the clustering of pixels. It follows that optimal design of α should maximize the between-groups variance with respect to the total variance $\check{\sigma}^2_Z$. Now, the major problem is the way of defining homogeneous groups of pixels. Owing to the univariate nature of the luminance, such groups can just be obtained on the basis of the peaks of the density of the original image. For example, looking at Figure 2(a), one can infer that 3 "homogeneous" regions are given by [0,90], [91,190], [191,255]. Given m intervals $(Z^*_{h-1}, Z^*_h]$, the between-groups variance is given by

$$\begin{aligned}\sigma_B^2 &= \sum_{h=1}^{m} \left(\bar{Z}_h - \bar{\bar{Z}}\,\right)^2 \frac{n_h}{n^2}\,, \qquad\qquad S_3(\alpha) = \frac{\check{\sigma}_B^2}{\check{\sigma}_Z^2} \\ \bar{Z}_h &= \frac{1}{n_h} \sum_{\{\,i,j\,:\,Z^*_{h-1} < Z_{ij} \leq Z^*_h\,\}} Z_{ij}\end{aligned} \tag{6}$$

where $\bar{Z}_h$ is the mean luminance of the h-th group, $\bar{\bar{Z}}$ is the overall mean, and n_h is the number of pixels in the h-th group. Maximizing the statistic (6) with respect α means optimizing the clustering, but respecting general features of the original image. In practice, the m-classes defined on the original density represent constraints for the sharpening, so that $S_3(\cdot)$ has a well definite maximum point.

The general feature of the statistics (4)-(6) is that they establish a trade-off between two *incompatible* cost (gain) functions, so that the resulting functional should have a well definite minimum (maximum). Figure 4 reports the values of $S_{1,2,3}(0.5 \leq \alpha \leq 7.5)$ computed on sharpened versions of the Lena image. Although the nature of these statistics is heuristic, the remarkable fact is that they agree in finding the optimal value of the coefficient, which is α=3.5. According to Figure 1, a slightly smaller value (say 3), may be preferable.

3. ADAPTIVE SHARPENING

Sharpening filters of type (2) have the undesirable side-effect of enhancing all noise components. This means that grain effects are produced also in uniform regions, where actual edges are absent. Moreover, because they weight neighboring pixels equally, the resulting transformation is insensitive to local contrast conditions. To alleviate these effects spatial autoregressive (SAR) models could be used and their parameters can be estimated adaptively.

With respect to the general scheme (1), SAR models can be used to estimate the gradient components $\hat{E}_{ij}$ in terms of residuals of regression. For a first order model, which potentially deals with all autocovariances $\gamma(h,k) \neq 0$, the representation is as follows (e.g. Grillenzoni, 2004)

$$Z_{ij} = \phi_1\, Z_{i,j-1} + \phi_2\, Z_{i-1,j} + \phi_3\, Z_{i-1,j-1} + \ldots + \phi_9\, Z_{i+1,j+1} + E_{ij} \quad (7)$$

where $\{\phi_k\}_1^9$ are coefficients to be estimated. With respect to the filter (2), where ϕ_k=1/9 all k, the adaptivity of the model (7) is evident.

Under conditions of stationarity one has $\gamma(0,1) = \gamma(0,-1)$ etc., so that the right hand side of (7) can be reduced to the first 3 terms only. This structure, which is called *causal*, enables the implementation of recursive forecasting algorithms, starting from suitable initial conditions on the upper-left border of the image. Computability of prediction errors is a necessary condition for the *parametric identifiability* of a SAR model (see Tjøsteim, 1983), which allows consistency to parameter estimates. Now, letting $\boldsymbol{\phi} = [\,\phi_1,\, \phi_2,\, \phi_3\,]'$ and $\boldsymbol{x}_{ij} = [\,Z_{i,j-1},\, Z_{i-1,j},\, Z_{i-1,j-1}\,]'$, the causal model can be written in regression form as $Z_{ij} = \boldsymbol{\phi}'\,\boldsymbol{x}_{ij} + E_{ij}$, and the least squares (LS) estimator becomes

$$\hat{\boldsymbol{\phi}}_{\text{LS}} = \arg\min_{\phi} \sum_{i=2}^{n}\sum_{j=2}^{n} E_{ij}^2(\boldsymbol{\phi}) = \left(\sum_{i=2}^{n}\sum_{j=2}^{n} \boldsymbol{x}_{ij}\boldsymbol{x}_{ij}'\right)^{-1} \sum_{i=2}^{n}\sum_{j=2}^{n} \boldsymbol{x}_{ij} Z_{ij} \quad (8)$$

Application of (8) to the Lena image provided $\hat{\boldsymbol{\phi}}_{\text{LS}} = [\,.57,\ .84,\ -.42\,]'$; with this, one can generate the residuals $\hat{E}_{ij}$, which provide the basis for the sharpening transformation (1). The design of the coefficient α can be subject to the same strategies as Section 2, namely to statistics (4)-(6). Indeed, numerical results are similar to those in Figure 4 and indicate the selection $\alpha = 3$. The implied sharpened image is shown in Figure 5 and is slightly better than Figure 1(d).

The adaptive capabilities of SAR models can be improved by applying *local* estimation techniques. These methods enable to obtain parameter estimates $\hat{\boldsymbol{\phi}}_{ij}$ which take into account local conditions of contrast and texture of the image. Following Grillenzoni (2004), a simple algorithm can be obtained from (8) by weighting the regressors with exponentially decaying weights

Fig. 5: Sharpened transformation of the Lena image obtained with a causal SAR(1) model.

$$\hat{\boldsymbol{\phi}}_{ij} = \left(\sum_{h=2}^{n} \sum_{k=2}^{n} \lambda_1^{|i-h|} \lambda_2^{|j-k|} \, \boldsymbol{x}_{hk} \, \boldsymbol{x}_{hk}' \right)^{-1} \sum_{h=2}^{n} \sum_{k=2}^{n} \lambda_1^{|i-h|} \lambda_2^{|j-k|} \, \boldsymbol{x}_{hk} \, Z_{hk} \quad (9)$$

where $0 < \lambda_1, \lambda_2 \leq 1$ are coefficients of spatial adaptivity.

Algorithm (9) is computational demanding, and its fastness can be improved with *recursive* algorithms which operate only by rows or by columns, such as

$$\begin{aligned} \hat{E}_{ij} &= Z_{ij} - \hat{\boldsymbol{\phi}}_{i,j-1}' \, \boldsymbol{x}_{ij} \\ \boldsymbol{R}_{ij} &= \lambda_2 \cdot \boldsymbol{R}_{i,j-1} + \boldsymbol{x}_{ij} \, \boldsymbol{x}_{ij}' \\ \hat{\boldsymbol{\phi}}_{ij} &= \hat{\boldsymbol{\phi}}_{i,j-1} + \boldsymbol{R}_{ij}^{-1} \, \boldsymbol{x}_{ij} \, \hat{E}_{ij} \end{aligned} \quad (10)$$

It is also advisable to vectorize the image as $\boldsymbol{z}$=vec($\boldsymbol{Z}$) (either by row or by column) and run the algorithm (10) starting both from the top and the bottom of $\boldsymbol{z}$. Estimates of type (9) can then be obtained by averaging the 4 resulting solutions. Figure 6 shows the result for the Lena image with λ=0.95.

Constraining $\lambda_1 = \lambda_2$, the resulting coefficient can be designed with bivariate forms of statistics (4)-(6). With respect to the skewness-kurtosis test and the Lena image, $S_1(\alpha, \lambda)$ attains a minimum at the point (4,0.5). However, given α, the quality of sharpened images is relatively insensitive to the choice of λ, and is similar to Figure 5. What drastically changes is the pattern of estimates $\hat{\boldsymbol{\phi}}_{ij}$, which contain useful information and require $\lambda > 0.9$ to be appreciated.

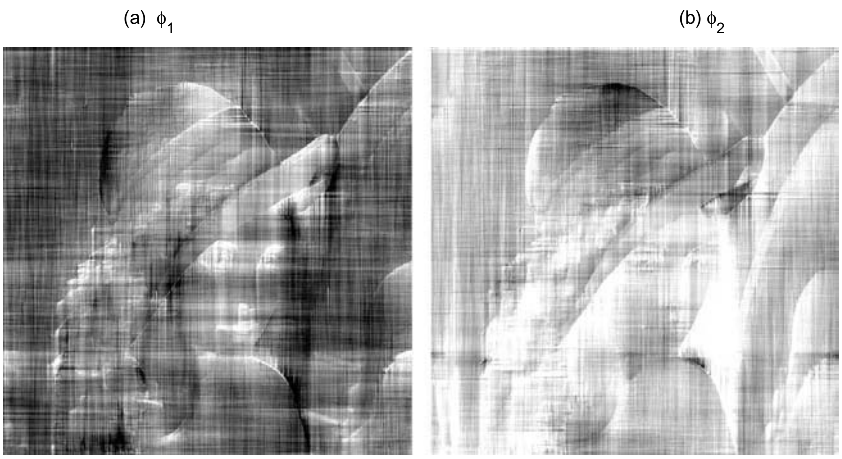

Fig. 6: Mean value of recursive estimates (10) obtained by rows (starting from left and right) and by columns (starting from top and bottom), with $\lambda = 0.95$.

In order to improve the quality of the image significantly, it is necessary to intervene on the mechanism of sharpening itself, by selecting the residuals (edges) to be added. A suitable approach is the opposite one of *robust* statistical methods; namely, trimming small residuals and enhancing the largest ones. In this way, uniform regions would be preserved from noise, and only contrasted regions would be enhanced. It is also possible to improve the smoothness in uniform regions by introducing a local filter which replaces the original pixels

Z_{ij} with the smoothed ones $\hat{Z}_{ij} = \hat{\boldsymbol{\phi}}_{\mathrm{LS}}' \boldsymbol{x}_{ij}$. Thus, using the indicator function $I(\cdot)$, the filter which simultaneously performs sharpening and smoothing transformations becomes

$$\tilde{Z}_{ij} = Z_{ij} + \alpha\, I\Big(|\hat{E}_{ij}| > \delta\, \hat{\sigma}_E\Big)\, \hat{E}_{ij} - I\Big(|\hat{E}_{ij}| \le \delta\, \hat{\sigma}_E\Big)\, \hat{E}_{ij} \tag{11}$$

which follows by the definition of $\hat{E}_{ij} = (Z_{ij} - \hat{Z}_{ij})$. Under Gaussianity, the value of δ is usually selected in the interval (1,3); however, since the density of E_{ij} has heavy tails the size of δ must be larger. In any event, the filter (11) has the tendency to smooth low contrast regions and produce sparse outliers.

Experimentally, the best visual performance on the Lena image was provided by a SAR filter with *adaptive* α-weights, such as

$$\begin{aligned} \check{Z}_{ij}^* &= Z_{ij} + \hat{\alpha}_{ij}\, \hat{E}_{ij}\,, \qquad \hat{\alpha}_{ij} = \alpha \left[\frac{\hat{\sigma}_{ij}}{\max(\hat{\sigma}_{ij})} \right] \\ \hat{\sigma}_{ij}^2 &= \frac{1}{(2d+1)^2} \sum_{h=-d}^{d} \sum_{k=-d}^{d} (Z_{i-h,j-k} - \bar{Z}_{ij})^2 \end{aligned} \tag{12}$$

where σ_{ij}^2 is a local variance of Z, and $\bar{Z}_{ij}$ is a local mean based on a $(2d{+}1)$ square window, with d=1, 2. The rationale underlying (12) is that the estimated edges (residuals) are enhanced proportionally to the local contrast of the original image. Because $\alpha_{ij} \le \alpha$, smooth regions are preserved from noise and outliers, while contrasted regions have weights near α.

The parameter α of (12) can be selected as in Section 2; however, the filter has shown less sensitivity to such coefficient with respect to non-adaptive methods. Figure 7(a) plots the weights $\hat{\alpha}_{ij}$ with $d = 1$, placed in increasing order and Figure 7(b) shows the path of the statistic (4). To increase the sensitivity of (12) to low-medium contrast, the profile of the weights α_{ij} can be made less convex by using α_{ij}^{δ}, $\delta < 1$. Finally, Figure 7(c) provides the sharpened image obtained with the optimum point $\alpha = 11$. As one can appreciate, its quality is significantly better than that of Figures 5 and 1(d).

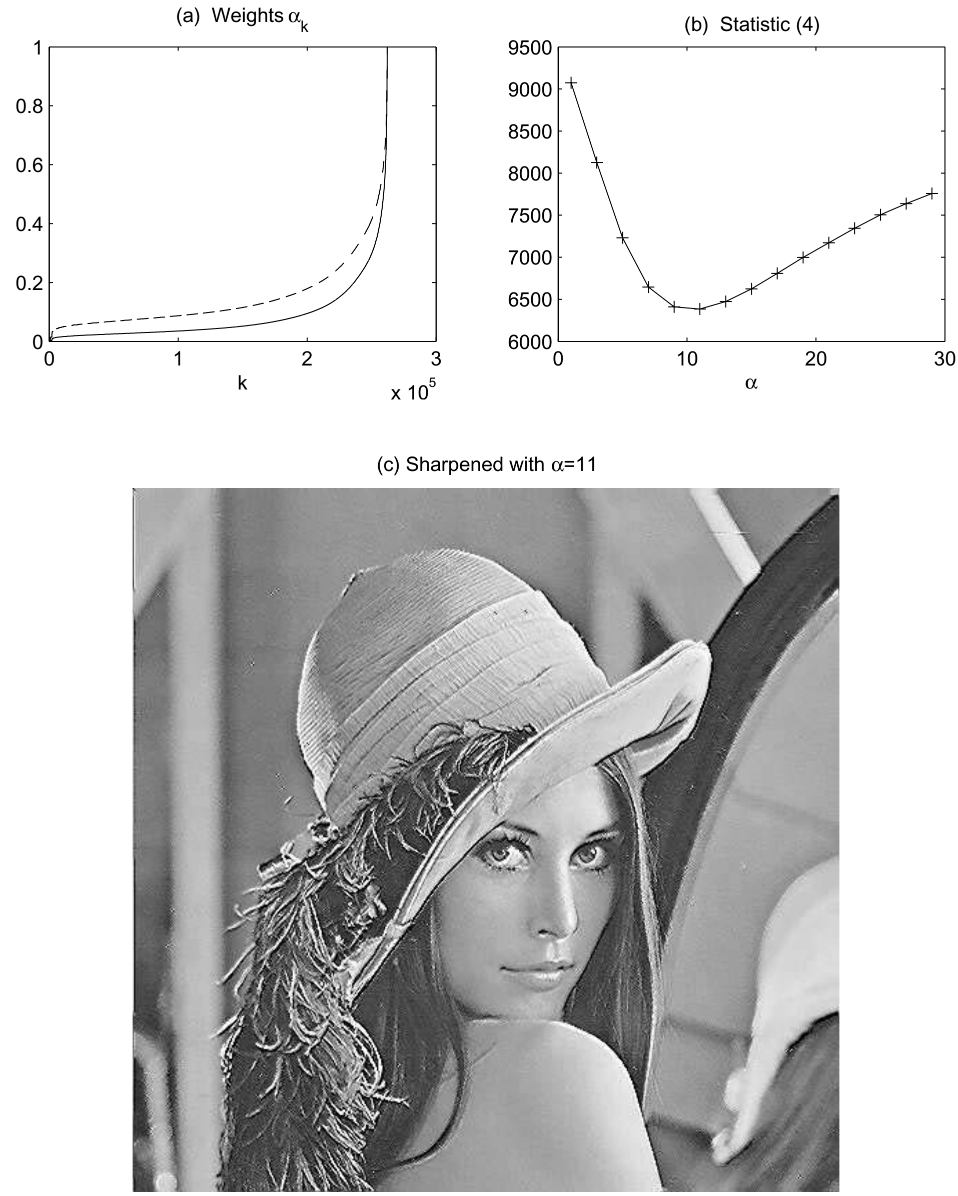

Fig. 7: Elements of the filter (12); (a) Weights $\hat{\alpha}_{ij}$ and $\hat{\alpha}_{ij}^{3/4}$ (dashed); (b) Statistic (4); (c) Sharpened image.

4. DISCUSSION

In this paper we have considered statistical methods of digital image enhancing. The two main contributions are: *i*) new techniques for the optimal design of existing methods (the so-called unsharp masking); and *ii*) new filters based on spatial autoregressive models (and their estimators).

In the first point we have developed 3 statistics of higher order moments (skewness, kurtosis, autocovariance, etc.) that behave in a strict convex (concave) manner with respect to the enhancing parameter. This behavior is due to their composite nature; in particular, they combine indicators that are sensitive only to sharpening or smoothing respectively. In this way, they tend to establish a trade-off between the components which characterize the image quality. At the experimental level, the remarkable fact is that all statistics have provided the same optimum point, and this comforts on their validity.

Usage of complex statistics is also present in the engineering literature. However, they are mostly employed for measuring the quality of compressed images, compared to the original ones (see Avcibas *et al.*, 2002), or for optimizing the auto-focusing in digital cameras and electron microscopes (e.g. Zhang *et al.*, 1999). In these cases mean square error (MSE) statistics would be sufficient.

In the second point we have changed the classical structure of unsharp masking filters, by replacing their edge components (usually based on local averages) with the prediction errors of SAR models. Local and recursive estimators for causal SAR models have been developed and their practical usage is demonstrated. We have also developed an adaptive approach for tuning sharpening weights on the basis of the local variance. This solves the problems of grain effect and noise diffusion which are present in classical sharpening techniques.

All the methods have been deeply tested on a well known GIF image used in image processing. Their validity is confirmed by the fact that final results (i.e. Figure 7) are comparable with best enhancing techniques recently proposed in engineering (e.g. Polesel *et al.* 2000, and Russo, 2005). At any rate, our methods have the advantage of a solid statistical background.

REFERENCES

AVCIBAS, I., SANKUR, B., SAYOOD, K. (2002). Statistical evaluation of image quality measures. *Jour. Electronic Imaging*, **11**, 206-223.

BERA, A.K., JARQUE, C.M. (1982). Model specification tests: a simultaneous approach. *Journal of Econometrics*, **20**, 59-82.

CAMPBELL T.G., DU BUF, J.M. (1990). A quantitative comparison of edge preserving smoothing. *Signal Processing*, **21**, 289-301.

CHU, C.K., GLAD, I., GODTLIEBSEN, F., MARRON, J.S. (1998). Edge-Preserving Smoothers for Image Processing. *Journal of American Statistical Association*, **93**, 526-541.

FUNT, B., CIUREA, F., McCANN, J. (2004). Retinex in Matlab. *Journal of Electronic Imaging*, **13**, 48 57.

GRILLENZONI, C. (2004). Adaptive spatio temporal models for satellite ecological data. *Journal of Agricultural, Biological and Environmental Statistics*, **9**, 158-180.

GUILLON, S., BAYLOU, P., NAJIM, M., KESKES, N. (1998). Adaptive nonlinear filters for 2D and 3D image enhancement. *Signal Processing*, **67**, 237-254.

HÄRDLE, W. (1991). *Smoothing Techniques: with Implementation in S.* Springer, Berlin.

POLESEL, A., RAMPONI, G., MATHEWS, J. (2000). Image enhancement via adaptive unsharp masking. *IEEE Transactions on Image Processing*, **9**, 505-510.

RUSSO, F. (2005). Automatic enhancement of noisy images using objective evaluation of image quality. *IEEE Trans. on Instrumentation and Measurement*, **54**, 1600-1606.

STARCK, J.L., MURTAGH, F., CANDES, E.J., DONOHO, D.L. (2003). Image contrast enhancement by curvelet transform. *IEEE Transactions on Image Processing*, **12**, 706-717.

TJØSTHEIM, D. (1983). Statistical Spatial Series Modeling II: Some Further Results on Unilateral Lattice Processes. *Advances in Applied Probability*, **15**, 562-584.

ZHANG, N.F., POSTECK, M.T., LARRABEE, R.D., VLADAR, A.E., KEERY, W.J., JONES, S.N. (1999). Image sharpness measurement in scanning electron microscope - Part III. *Scanning*, **21**, 246-252.

UN APPROCCIO STATISTICO AL MIGLIORAMENTO DELLA NITIDEZZA DELLE IMMAGINI

Riassunto

Nella letteratura ingegneristica sono stati proposti diversi metodi per il miglioramento della qualità delle immagini. Il loro maggiore inconveniente è dato dal fatto che la loro regolazione viene sviluppata con regole di buon senso o valutazioni soggettive. Questo articolo sviluppa tecniche statistiche per l'ottimizzazione della nitidezza delle immagini. La caratteristica più rilevante è rappresentata dalla selezione automatica del coeciente che controlla l'addizione del gradiente. L'approccio è basato su misure statistiche che stabiliscono un interscambio tra tra perequazione e nitidezza. Più in generale, altri classici possono essere sostituiti da modelli autoregressivi spaziale i cui coecienti possono essere stimati col metodo dei minimi quadrati adattivi. Una estesa applicazione su una nota immagine test dimostra la validità delle soluzioni proposte.

Parole Chiave: Identicazione d'Impronte, Miglioramento di Qualità, DensitàNucleari, Minimi Quadrati, Test di Normalità, Modelli Autoregressivi Spaziali.

ACKNOWLEDGMENTS

This work was supported by the MIUR PRIN Grant n. 2005134530-002.